Technology in Cancer Research & Treatment
Volume 23: 1-12

DOI: 10.1177/15330338241246649
journals.sagepub.com/home/tct

Study on the Role and Mechanism of SLC3A2 in Tumor-Associated Macrophage Polarization and Bladder Cancer Cells Growth

Peishan Wu, MS[1], Lingna Zhao, MS[1], Guangqi Kong, BD[1], and Bo Song, MD[1]

Abstract

Background: Solute carrier family 3 member 2 (SLC3A2) is highly expressed in various types of cancers, including bladder cancer (BLCA). However, the role and mechanism of SLC3A2 in the onset and progression of BLCA are still unclear. **Methods:** The interfering plasmid for SLC3A2 was constructed and transfected into BLCA cells. Cell proliferation, invasion, and migration abilities were assessed to evaluate the impact of SLC3A2 silencing on BLCA cell growth. M1 and M2 macrophage polarization markers were detected to evaluate macrophage polarization. The levels of reactive oxygen species (ROS), lipid peroxidation, and Fe^{2+}, as well as the expression of ferroptosis-related proteins, were measured to assess the occurrence of ferroptosis. Ferroptosis inhibitors were used to verify the mechanism. **Results:** The experimental results showed that SLC3A2 was highly expressed in BLCA cell lines. The proliferation, invasion, and migration of BLCA cells were reduced after interfering with SLC3A2. Interference with SLC3A2 led to increase the expression of M1 macrophage markers and decreased the expression of M2 macrophage markers in M0 macrophages co-cultured with tumor cells. Additionally, interference with SLC3A2 led to increased levels of ROS, lipid peroxidation, and Fe^{2+}, downregulated the expression of solute carrier family 7 member11 (SLC7A11) and glutathione peroxidase 4 (GPX4), while upregulated the expression of acyl-coA synthetase long chain family member 4 (ACSL4) and transferrin receptor 1 (TFR1) in BLCA cells. However, the impact of SLC3A2 interference on cell proliferation and macrophage polarization was impeded by ferroptosis inhibitors. **Conclusion:** Interference with SLC3A2 inhibited the growth of BLCA cells and the polarization of tumor-associated macrophages by promoting ferroptosis in BLCA cells.

Keywords

bladder cancer, SLC3A2, cell growth, macrophage polarization, ferroptosis

Abbreviations

ANOVA, analysis of variance; BCA, bicinchoninic acid; BSA, bovine serum albumin; BLCA, bladder cancer; CM, conditioned medium; DAPI, 4',6-diamidino-2-phenylindole; FBS, fetal bovine serum; FITC, fluorescein isothiocyanate; INF-γ, Interferon-γ; iNOS, inducible nitric oxide synthase; LPS, lipopolysaccharide; mTOR, mammalian target of rapamycin; OD, optical density; PBS, Phosphate buffer saline; PFA, paraformaldehyde; PGSK, Phen Green SK; PMA, 12-O-tetradecanoylphorbol-13-acetate; PVDF, polyvinylidene fluoride; RIPA, radio-immunoprecipitation assay; ROS, reactive oxygen species; SD, standard deviation; SDS-PAGE, sodium dodecyl sulfate - polyacrylamide gel electrophoresis; sh-NC, shRNA-normal control; SLC, solute carriers; TBARS, thiobarbituric acid reactive substance; TME, tumor microenvironment; TBST, tris buffered saline with tween-20; qRT-PCR, quantitative real-time PCR; VEGFA, vascular endothelial growth factor A; WB, western blot

Received: December 5, 2023; Revised: February 5, 2024; Accepted: March 18, 2024.

Introduction

Bladder cancer (BLCA) is among the prevalent tumors affecting the urinary system, ranking as the 7th most common cancer globally.[1] BLCA, being a malignant tumor, is characterized by its aggressive invasiveness and tendency for recurrence.[2]

[1] Department of Urology, Beijing Luhe Hospital, Capital Medical University, Beijing, China

Corresponding Author:
Bo Song, Department of Urology, Beijing Luhe Hospital, Capital Medical University, Beijing 101117, China.
Email: songbodoc11@163.com

Reports indicate approximately 549,000 new cases of BLCA annually, resulting in 200,000 deaths.[3] The prevalent form of BLCA is the invasive type, which extends to the muscle layer, with only 50% of such cases being surgically curable. The remaining patients are deemed incurable due to the disease's highly invasive nature.[4,5]

The tumor microenvironment (TME) encompasses noncancerous cells within a tumor along with the factors they generate and release.[6] Interactions between tumor cells and the TME critically influence tumorigenesis, progression, metastasis, and therapy response.[7] Macrophages constitute a significant component of the TME. Within the TME, macrophages can polarized into M1 or M2 types,[8] exhibiting opposite roles. Inhibiting M2 macrophage polarization effectively hinders tumor growth and metastasis.[9] Ferroptosis, an iron-dependent, nonapoptotic cell death mechanism, is noteworthy in cancer due to the higher iron demand for tumor cell proliferation, making them more susceptible to iron-catalyzed necrosis.[10] Therefore, ferroptosis has garnered considerable attention as a potential therapeutic approach for cancer treatment. Numerous ferroptosis-proteins have been identified in BLCA specimens,[11] indicating its important role in BLCA development. In addition, studies demonstrate crosstalk between ferroptosis and TME, with macrophage polarization disrupting the TME and inducing ferroptosis in cancer cells.[12] Furthermore, ferroptosis activation induces M1 polarization and inhibits M2 polarization within TME, consequently retarding cancer progression.[13] Hence, the interplay between ferroptosis and macrophages has been employed in researching diverse cancer treatments.[14]

Solute carrier family 3 member 2 (SLC3A2), the prototypical member of the solute carriers (SLC) family, exhibits high expression levels in numerous malignant tumor cells.[15] Knockdown of SLC3A2 in lung adenocarcinoma cells inhibits M2 polarization in macrophages.[16] In colorectal cancer, suppressing SLC3A2 expression hampers cancer cell proliferation, migration, and invasion via ferroptosis induction.[17] Reports indicate that SLC3A2 is highly expressed in tumor tissues of patients with BLCA, correlating with poor prognosis.[18] However, the precise role of SLC3A2 in BLCA development remains nebulous.

Therefore, based on existing reports, this study delved into the expression of SLC3A2 in BLCA cells and the underlying mechanisms in cancer progression. The results showed that the expression of SLC3A2 in BLCA cells was elevated, and SLC3A2 silencing inhibited BLCA cell proliferation, invasion, and migration, along with reduced M2 macrophage polarization. The observed effects were linked to the promotion of ferroptosis following SLC3A2 silencing in BLCA cells.

Materials and Methods

Ethical Approval

This research has been reviewed by the Ethics Committees of Beijing Luhe Hospital, Capital Medical University. It does not involve human tissue/samples or animal experiments. Therefore, this research does not require approval from the Ethics Committee.

Prediction of SLC3A2 Expression and Prognostic Correlation

Assessment of SLC3A2 expression in BLCA was conducted through the UALCAN website (https://ualcan.path.uab.edu/analysis.html). Initial examination of SLC3A2 gene with prognosis in BLCA was analyzed through the UALCAN website and Kaplan-Meier Plotter websites (https://kmplot.com/analysis/).

Cell Culture

The human normal bladder epithelial cell line SV-HUC-1 and the human monocytic leukemia (THP-1) cell line were purchased from the Type Culture Collection of the Chinese Academy of Sciences. The human BLCA cell lines 5637 and J82 were purchased from Sunncell, and T24 and UM-UC-3 were purchased from the National Platform of Experimental Cell Resources for Sci-Tech, Cell Resource Center. The SV-HUC-1, UM-UC-3, and J82 cell lines were cultured in DMEM medium (Gibco). THP-1, 5637, and T24 cells were cultured in RPMI-1640 medium (Gibco). The culture media were supplemented with 10% fetal bovine serum (FBS), Thermo Fisher Scientific) and 1% penicillin-streptomycin. Cells were cultured under culture conditions of 37 °C with 5% CO_2 incubator.

Cell Transfection

GenePharma designed and synthesized the shRNA targeting SLC3A2 (shRNA-SLC3A2-1/2) and the corresponding shRNA-negative control (shRNA-NC). When cells had grown to 60% to 80% confluence, cells underwent transfection using the Lipofectamine 2000 reagent (Invitrogen) following the recommended protocol. Subsequently, cell harvesting for further analysis occurred 48 h after transfection.

Cell Counting Kit-8 (CCK8) Assay

The inoculation of cells (5×10^3 cells/mL) into 96-well plates was initially conducted, after which was the cultivation for 24, 48, and 72 h. Afterwards, 10 μL of WST-8 (Beyotime) was put into each well to further cultivate the plates for 2 h. With the help of a microplate reader, the absorbance was resolved at 450 nm. All experiments were replicated 5 times.

5-Ethynyl-2-Deoxyuridine Staining

Cell proliferation was detected utilizing the 5-ethynyl-2-deoxyuridine (EDU) kit (RiboBio). EDU and 4',6-diamidino-2-phenylindole (DAPI) working solutions were proportionally diluted with complete cell medium according to the manufacturer's instructions. Briefly, the transfected cells were incubated

in the medium containing EDU working solution for 6 h, then washed with phosphate buffer saline (PBS), fixed, permeabilized and washed again, and incubated with DAPI solution for 10 min in the absence of light. Image acquisition was performed using a fluorescence microscope (Nikon). All experiments were replicated 3 times.

Colony Formation Assay

For clone formation, transfected BLCA cells were digested using trypsin (C0201, Beyotime), re-suspended, and counted. An equal number of BLCA cells was subsequently plated into a 3.5 cm well. Following 14 days of culture in complete medium, crystal violet was used to stain visible colonies. Finally, stained colonies were photographed, counted, and compared among different groups. All experiments were replicated 3 times.

Wound Healing

Transfected cells were inoculated into 6-well plates, and upon confluence, the cell layer was gently scraped with a sterile plastic pipette. Subsequently, cells were cultured in FBS-deficient medium, and electron microscopy images were captured at 0 and 24 h. Cell migratory capacity was assessed by measuring the change in the size of the wounded area. All experiments were replicated 5 times.

Transwell

Transfected cells were cultured in serum-free medium in the upper chamber of Transwell filter membranes precoated with Matrigel, while the lower chamber contained medium supplemented with 10% **FBS**. After 24 h of incubation at 37 °C in a cell culture incubator containing 5% CO_2, cells in the upper chamber were removed. Subsequently, cells were fixed in methanol for 15 min, stained with crystal violet for 20 min, photographed in 5 random fields of view under a microscope (×200), and counted. All experiments were replicated 5 times.

Macrophage Polarization Induction and Co-Culture

THP-1 was treated with 100 ng/mL (12-O-tetradecanoylphorbol-13-acetate (PMA), Sigma Aldrich) for 24 h to differentiate into M0 macrophages. After differentiation into M0 macrophages, (lipopolysaccharide (LPS), 10 pg/mL) and (interferon-γ (INF-γ), 20 ng/mL) were added to stimulate the cells for 24 h to induce M1-type macrophage polarization. IL-4 (20 ng/mL) and IL-13 (20 ng/mL) were added to stimulate the cells to induce M2-type macrophage polarization. Collect T24 cell culture medium from different experimental groups as conditioned medium (CM). M0 macrophages were stimulated using CM for 48 h, then M0 macrophages were harvested to detect the effect of BLCA cells on M0 macrophage polarization.[19]

Immunofluorescent Staining

Double CD68/iNOS and CD68/CD206 immunofluorescence staining was used to identify M1 and M2 macrophages, respectively. M0 macrophages were cultured on slides and then fixed with 4% paraformaldehyde (PFA) at room temperature. The cells were then permeabilized with 0.05% Triton X-100 and blocked with 5% (bovine serum albumin (BSA), Solarbio) for 1 h. Then, the cells were incubated with primary antibodies: CD68 (ab955, Abcam, 1:200 dilution), (inducible nitric oxide synthase (iNOS), ab15323, Abcam, 1:100 dilution), CD206 (ab64693, Abcam, 1:100 dilution) overnight at 4 °C. DAPI was used for nuclear staining. Fluorescence microscopy was used to visualize immunofluorescence. All experiments were replicated 3 times.

Ferroptosis Detection

In accordance with the manufacturer's instructions, we utilized BODIPY 581/591 C11 (Thermo Fisher) staining to identify reactive oxygen species (ROS) within the cells. Fluorescence imaging was performed using Texas red (590 nm) and fluorescein isothiocyanate (FITC) (510 nm) emission filters. Lipid peroxidation levels in cells were determined using the thiobarbituric acid reactive substance (TBARS) assay kit (Biyun Tian), and detected the results colorimetrically at 532 nm. Cellular Fe^{2+} levels were assessed through the Phen Green SK (PGSK) fluorescent probe assay (Chemstan, China). Ferrostatin-1 (Fer-1, 10 μM), an ferroptosis inhibitor, was pretreated for mechanism validation. All experiments were replicated 5 times.

Western Blot Assay

Cells were lysed with radio-immunoprecipitation assay (RIPA) buffer (PC101, Epizyme) containing protease inhibitors to extract total proteins, and bicinchoninic acid (BCA) protein assay kit (ZJ102, Epizyme) was used for protein quantification. Equivalent amounts of proteins (20 μg) from each group were loaded onto 10% sodium dodecyl sulfate - polyacrylamide gel electrophoresis (SDS-PAGE) gels (G2003-50 T, Servicebio) and then transferred to polyvinylidene fluoride (PVDF) membranes. Membranes were incubated overnight at 4 °C with primary antibodies, including GAPDH antibody (AF7021, Affinity, 1:1000 dilution), SLC3A2 antibody (A19880, Abclonal, 1:800 dilution), SLC7A11 antibody (DF12509, Affinity, 1:1100 dilution), GPX4 antibody (DF6701, Affinity, 1:1000 dilution), ACSL4 antibody (ab155282 Abcam, 1:1500 dilution), and TFR1 antibody (A5865, Abclonal, 1:1000 dilution). After washing with tris buffered saline with Tween-20 (TBST), the membranes were incubated with a secondary antibody Goat Anti-Rabbit IgG (S0001, Affinity, 1:5000 dilution) for 2 h at 37 °C. Signals were detected using a chemiluminescence system (Millipore) and ImageJ software was utilized

Table 1. Primer Sequences.

Gene	Primer	Sequences (5′-3′)
GAPDH	Forward	GGAGCGAGATCCCTCCAAAAT
	Reverse	GGCTGTTGTCATACTTCTCATGG
SLC3A2	Forward	CTGGTGCCGTGGTCATAATC
	Reverse	GCTCAGGTAATCGAGACGCC
CCL2	Forward	CAGCCAGATGCAATCAATGCC
	Reverse	TGGAATCCTGAACCCACTTCT
CCL4	Forward	CTGTGCTGATCCCAGTGAATC
	Reverse	TCAGTTCAGTTCCAGGTCATACA
IL-23A	Forward	CTCAGGGACAACAGTCAGTTC
	Reverse	ACAGGGCTATCAGGGAGCA
IL-10	Forward	TCAAGGCGCATGTGAACTCC
	Reverse	GATGTCAAACTCACTCATGGCT
VEGFA	Forward	AGGGCAGAATCATCACGAAGT
	Reverse	AGGGTCTCGATTGGATGGCA
Arg-1	Forward	TGGACAGACTAGGAATTGGCA
	Reverse	CCAGTCCGTCAACATCAAAACT

for the quantification of immunoblotting signals. All experiments were replicated 3 times.

RNA Extraction and Quantitative Real-Time PCR

Cellular RNA extraction was extraction was carried out utilizing TRIzol (Invitrogen). Reverse transcription of complementary DNA (cDNA) was performed using the PrimeScriptTM RT Kit (Toyobo). Subsequently, the cDNA samples underwent real-time quantitative polymerase chain reaction using a real-time PCR reaction system (Biorad). GAPDH was used as an internal reference, and relative messenger RNA (mRNA) expression levels were determined by the $2^{-\Delta\Delta CT}$ method. Primer sequences were obtained from PrimerBank and were listed in Table 1. All experiments were replicated 3 times.

Statistical Analysis

Experimental data were expressed as mean ± standard deviation and analyzed with GraphPad Prism 8 (GraphPad Software Inc.). One-way analysis of variance was used to compare the difference between multiple groups. $P < .05$ was defined as statistically significant.

Results

SLC3A2 Expression is Significantly Higher in BLCA Tissues and Cells

Online database analysis results indicated that the SLC3A2 in BLCA tissues (n = 408) was significantly higher than that in the control group (n = 19) (Figure 1A). Additionally, the results showed a significant correlation between SLC3A2 overexpression and a poorer prognosis in patients with BLCA (Figure 1BC). Subsequently, we examined the expression of SLC3A2 in BLCA cell lines. Our findings indicated a substantial increase in both mRNA level (Figure 1D, $P < .001$) and protein expression (Figure 1E, $P < .01$) of SLC3A2 in BLCA cell lines compared to normal bladder epithelial cells. Among them, T24 BLCA cells exhibited the highest expression of SLC3A2. Consequently, T24 cells were chosen for further investigations.

Interference With SLC3A2 Inhibits BLCA Cell Proliferation, Invasive, and Migration

Next, an interference plasmid targeting SLC3A2 was constructed and its efficacy evaluated. Results indicated superior interference efficiency with sh-SLC3A2-1 was compared to sh-SLC3A2-2 (Figure 2A and B, $P < .001$). Consequently, T24 cells were transfected with sh-SLC3A2-1. The proliferation assay showed a significant decrease in cell OD value (Figure 2C, $P < .001$), attenuation in EDU fluorescence intensity (Figure 2D), and a reduction in cell colony formation (Figure 2E, $P < .001$) in the sh-SLC3A2 group compared to the control and shRNA-normal control (sh-NC). Additionally, wound healing and Transwell assays revealed a decrease in cell migration (Figure 2F, $P < .001$) and invasive ability (Figure 2G, $P < .001$) in the sh-SLC3A2 group.

Interference With SLC3A2 Inhibits M2-Type Polarization of Tumor-Associated Macrophages

M0 macrophages underwent polarization upon exposure to diverse inducers, and the expression of M1 and M2 markers was subsequently assessed. The results showed a significant increase in the levels of M1-type markers CCL2, CCL4, and IL-23A after LPS and INF-γ induction (Figure 3A, $P < .05$), accompanied by enhanced fluorescence intensity of M1-type macrophage markers CD68/iNOS (Figure 3B). Following IL-4 and IL-13 induction, a significant elevation in the levels of M2-type markers IL-10, VEGFA, and Arg-1 was observed (Figure 3A), accompanied by enhanced fluorescence intensity of the M2-type macrophage marker CD68/CD204 (Figure 3C).

Next, M0 macrophages were stimulated with CM from T24 cells, revealing a significant increase in M1-type marker mRNA levels and a significant decrease in M2-type marker mRNA levels in the sh-SLC3A2 group (Figure 3D, $P < .001$). In addition, the sh-SLC3A2 group exhibited increased fluorescence intensity of the M1-type macrophage marker CD68/iNOS (Figure 3E) and decreased fluorescence intensity of the M2-type macrophage marker CD68/CD204 (Figure 3F) compared to the control and sh-NC groups.

Interference With SLC3A2 Promotes Ferroptosis in BLCA Cells

The BODIPY 581/591 C11 fluorescent probe showed a progressive elevation in lipid ROS levels in T24 cells of the sh-SLC3A2 group (Figure 4A). In addition, the production of TBARS (Figure 4B, $P < .001$) and the cellular Fe^{2+} concentration (Figure 4C) were significantly increased in macrophages in the sh-SLC3A2 group compared to the control and sh-NC

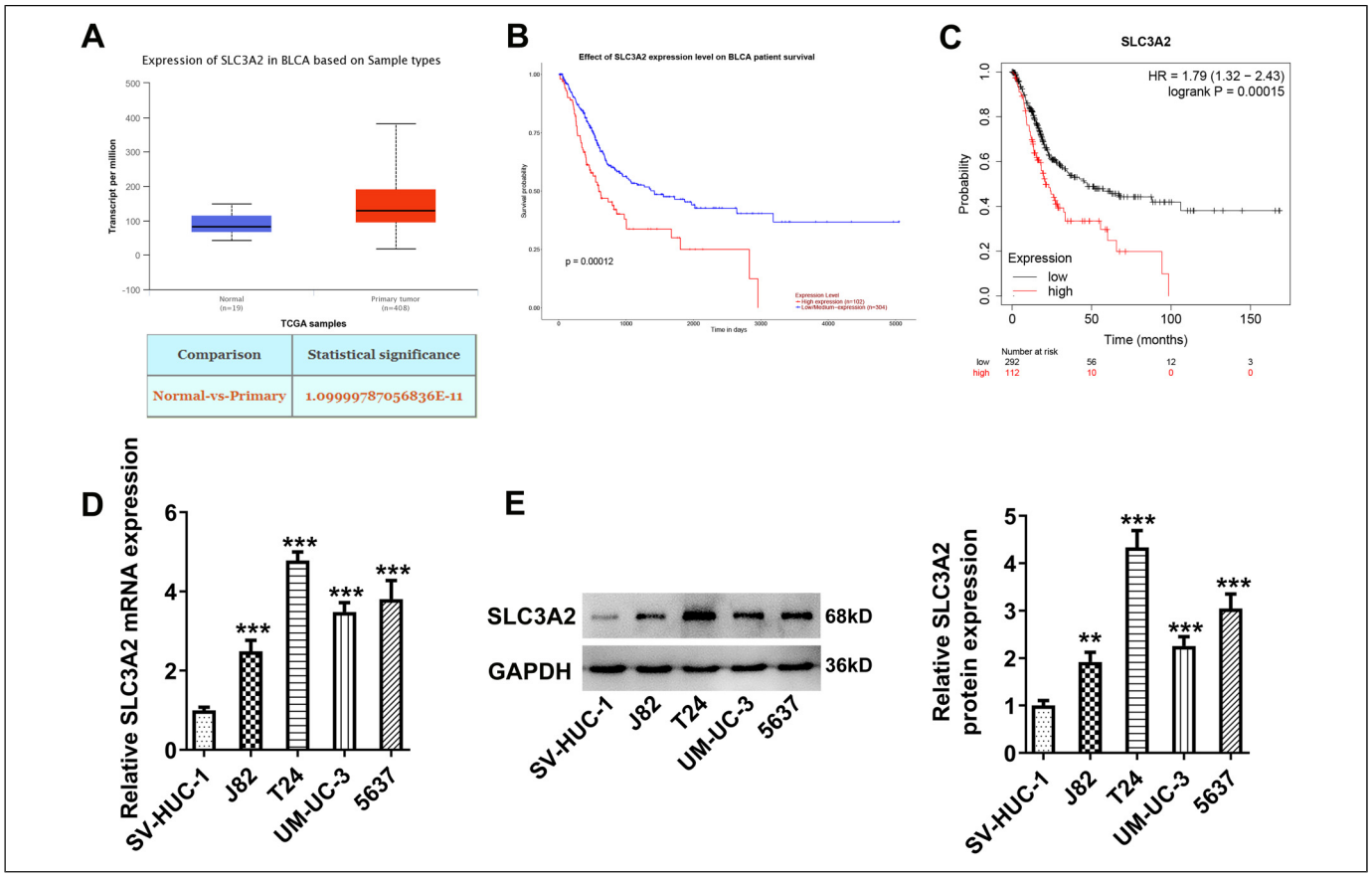

Figure 1. The expression of SLC3A2 is significantly higher in BLCA tissues and cells. The expression of SLC3A2 in BLCA tissues (n = 408) and normal tissue (n = 19) (A). The correlation between SLC3A2 and the prognosis of patients with BLCA by UALCAN database (B). The correlation between SLC3A2 and the prognosis of patients with BLCA by Kaplan-Meier Plotter website (C). mRNA expression levels of SLC3A2 in different BLCA cell lines (D, n = 3). Protein expression levels of SLC3A2 in different BLCA cell lines (E, n = 3). $^{**}P < .01$, $^{***}P < .001$ versus SV-HUC-1. Abbreviations: BLCA, bladder cancer; mRNA, messenger RNA.

groups. Western blot (WB) analysis indicated a reduction in the protein expression of LC7A11 and GPX4 in the sh-SLC3A2 group, accompanied by an elevation in the protein expression of ACSL4 and TFR1 (Figure 4D, $P < .001$).

Interference With SLC3A2 Inhibits BLCA Cell Proliferation, Invasive, and Migration by Promoting Ferroptosis

Next, we performed mechanistic validation utilizing the ferroptosis inhibitor Fer-1. The results demonstrated the ferroptosis inducer mitigated the inhibitory effect of SLC3A2 silencing on cellular proliferative capacity, as evidenced by elevated optical density (OD) (Figure 5A, $P < .001$), enhanced EDU fluorescence (Figure 5B), and increased cell colony formation (Figure 5C, $P < .01$) in the Fer-1 + sh-SLC3A2 group in comparison to the sh-SLC3A2 group. Meanwhile, wound healing and Transwell assays revealed that the application of Fer-1 augmented cell migration (Figure 5D, $P < .001$) and invasion ability (Figure 5E, $P < .001$) compared to the sh-SLC3A2 group.

Interference With SLC3A2 Inhibits M2-Type Polarization of Tumor-Associated Macrophages by Promoting Ferroptosis

Finally, we reassessed the polarization of M0 macrophages following ferroptosis inhibitor application. The results showed a significant reduction in the levels of M1-type markers CCL2 ($P < .001$), CCL4 ($P < .001$), and IL-23A ($P < .01$), alongside a significant increase in the levels of M2-type markers IL-10 ($P < .001$), vascular endothelial growth factor A (VEGFA) ($P < .01$), and Arg-1 ($P < .01$) in the Fer-1 + sh-SLC3A2 group compared to the sh-SLC3A2 group (Figure 6A). Immunofluorescence results demonstrated a decrease in the fluorescence intensity of the M1-type macrophage marker CD68/iNOS (Figure 6B), along with an increase in the fluorescence intensity of the M2-type macrophage marker CD68/CD204 (Figure 6E) in the Fer-1 + sh-SLC3A2 group.

Discussion

BLCA is the most prevalent malignancy affecting the urinary system. Utilizing an online database, this study aimed to

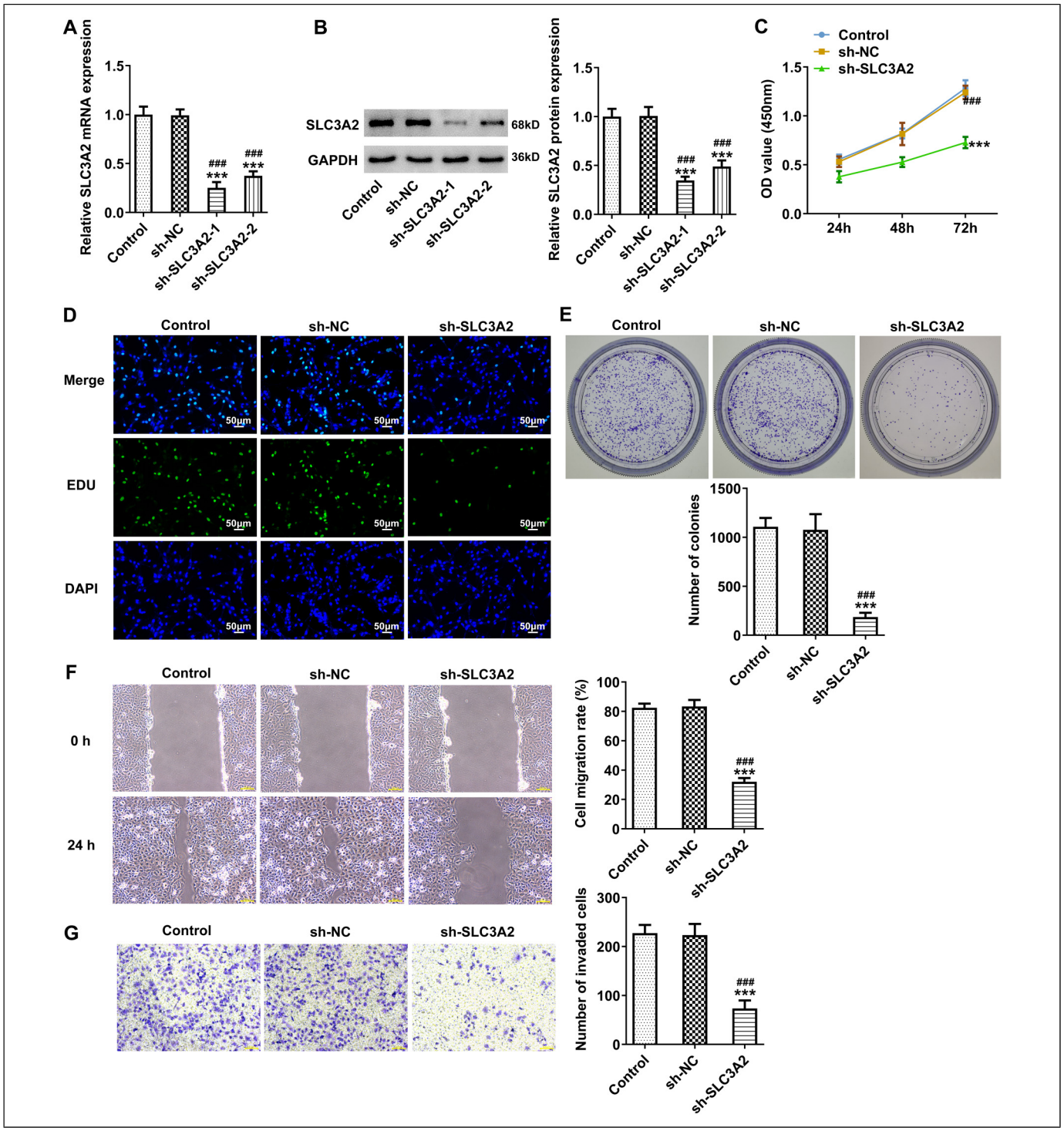

Figure 2. Interference with SLC3A2 inhibits BLCA cell proliferation, invasive, and migration. qRT-PCR assay for plasmid interference effects assay (A, n = 3). WB assay for plasmid interference effects assay (B, n = 3). Cell proliferation detection by CCK8 assay (C, n = 5). Cell proliferation detection by EDU staining (D, n = 3). Cell proliferation detection by Colony formation assay (E, n = 3). Cell migration detection by wound healing assay (F, n = 5). Cell invasion detection by Transwell assay (G, n = 5). $^{***}P < .001$ versus control; $^{\#\#\#}P < .001$ versus sh-NC. Abbreviations: BLCA, bladder cancer; EDU, 5-ethynyl-2-deoxyuridine; qRT-PCR, quantitative real-time PCR; WB, western blot.

predict and analyze the expression of SLC3A2 in T24 BLCA cells. Furthermore, experimental investigations, were conducted to explore the potential role of SLC3A2 in the development of BLCA. Research findings reveal a significant upregulation of SLC3A2 in both BLCA tissues and cells, correlating with an unfavorable prognosis. Interfering with the

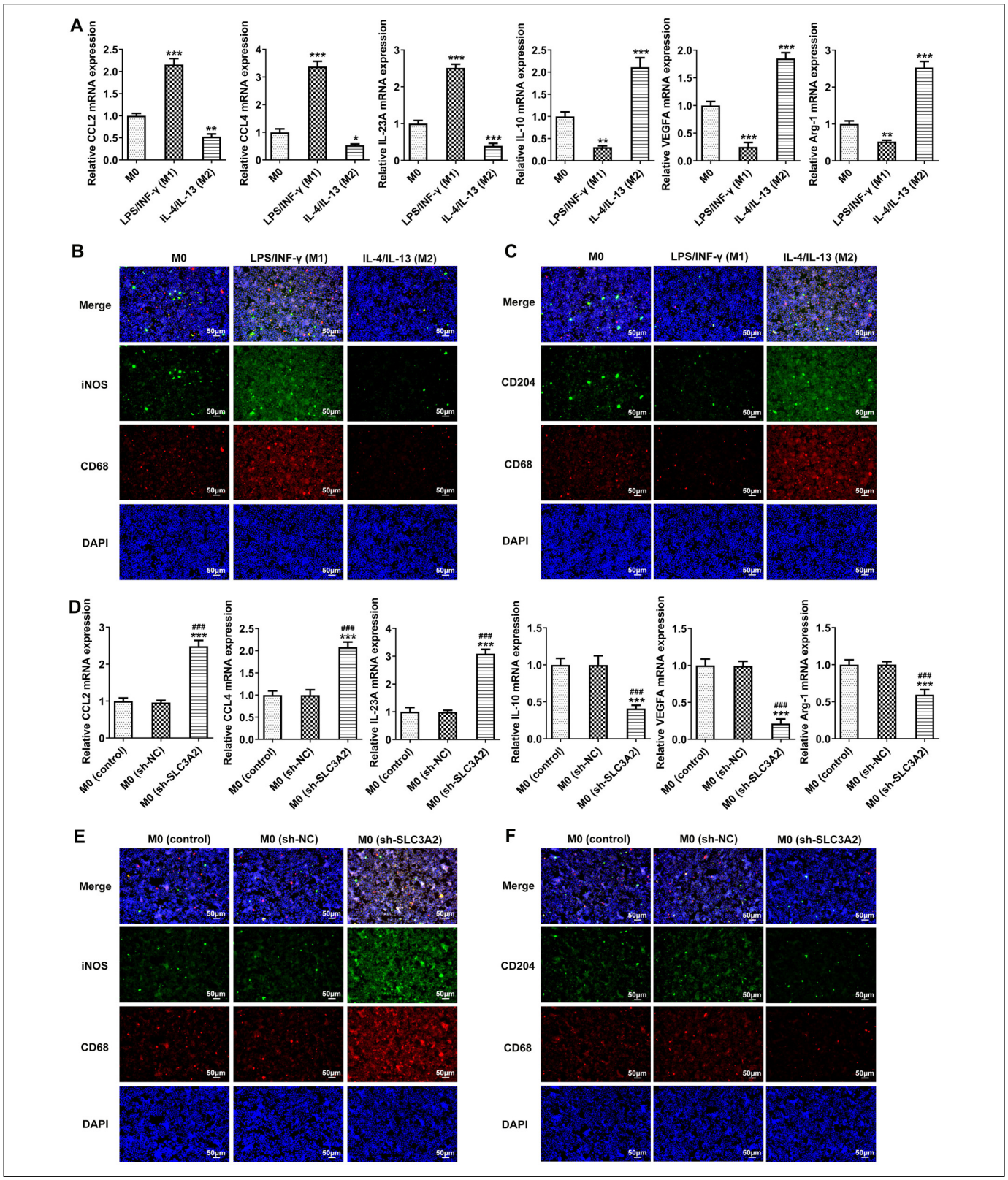

Figure 3. Interference with SLC3A2 inhibits M2-type polarization of tumor-associated macrophages. M1 and M2 type markers in macrophages detection, $^{*}P < .05$, $^{**}P < .01$, $^{***}P < .001$ versus M0 (A, n = 3). Double immunofluorescence staining of M1 macrophage markers (B, n = 3). Double immunofluorescence staining of M2 macrophage markers (C, n = 3). M1 and M2 type markers expression in macrophages after CM stimulation, $^{***}P < .001$ versus control; $^{\#\#\#}P < .001$ versus sh-NC (D, n = 3). Double immunofluorescence staining of M1 macrophage markers after CM stimulation (E, n = 3). Double immunofluorescence staining of M2 macrophage markers after CM stimulation (F, n = 3). Abbreviation: CM, conditioned medium.

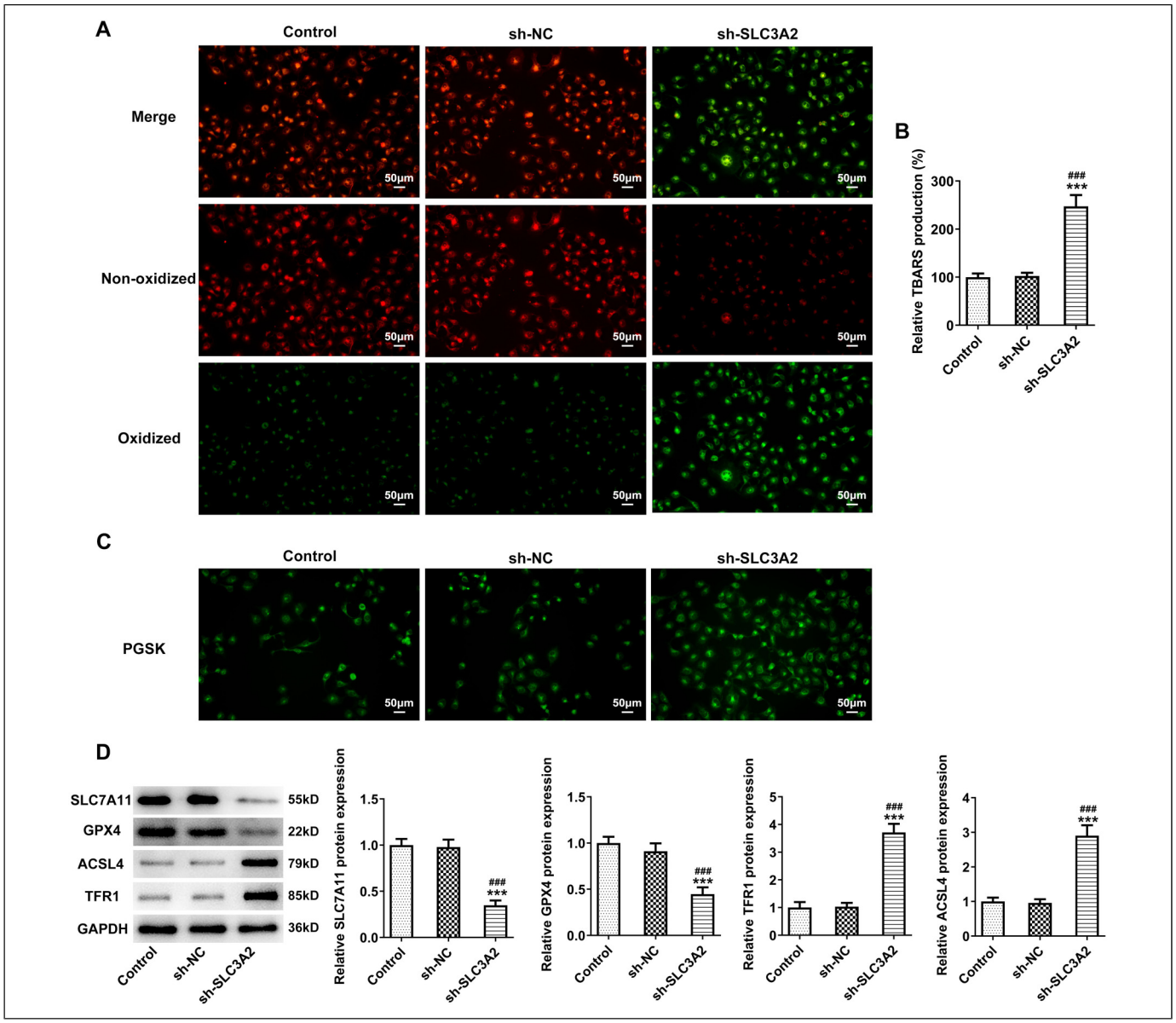

Figure 4. Interference with SLC3A2 promotes ferroptosis in BLCA cells. BODIPY 581/591 C11 staining (A, n = 5). Determination of TBARS production rate (B, n = 5). PGSK fluorescent probe (C, n = 3). WB assay for detecting the expression of ferroptosis-related proteins in cells (D, n = 3). ***$P < .001$ versus control; $^{###}P < .001$ versus sh-NC. Abbreviations: BLCA, bladder cancer; PGSK, Phen Green SK; TBARS, thiobarbituric acid reactive substance; WB, western blot.

expression of SLC3A2 induces ferroptosis, thereby impeding the proliferation of BLCA cells and preventing M2 polarization in tumor-associated macrophages.

The upregulation of SLC3A2 has been reported to be documented across various malignant tumors. Xiao et al[18] identified elevated expression of SLC3A2 in tumor tissues of patients with BLCA by bioinformatics analysis, correlating it with an unfavorable prognosis. These findings align with the results obtained from our online database analysis. Additionally, a recent study reported the involvement of SLC3A2 in nonprimary BLCA. The study found that knocking out SLC3A2 significantly inhibited the proliferation, migration, and invasion of MC SV-HUC T2 cells.[20] This study experimentally investigated the role of SLC3A2 BLCA cells for the first time. However, primary BLCA is more common compared to nonprimary BLCA.[21] T24 cells are a type of human bladder transitional cell carcinoma cells, which make up over 90% of BLCA.[22] Therefore, investigating the role of SLC3A2 in primary BLCA, particularly in transitional cell carcinoma, is highly valuable for understanding the involvement of SLC3A2 in BLCA. This study revealed that inhibiting the expression of SLC3A2 in T24 cells suppressed the proliferation, invasion, and migration of cancer cells. This suggests that SLC3A2 functions as an oncogene in both primary and nonprimary BLCA. Furthermore, this study delved deeper into the mechanism of how interfering with

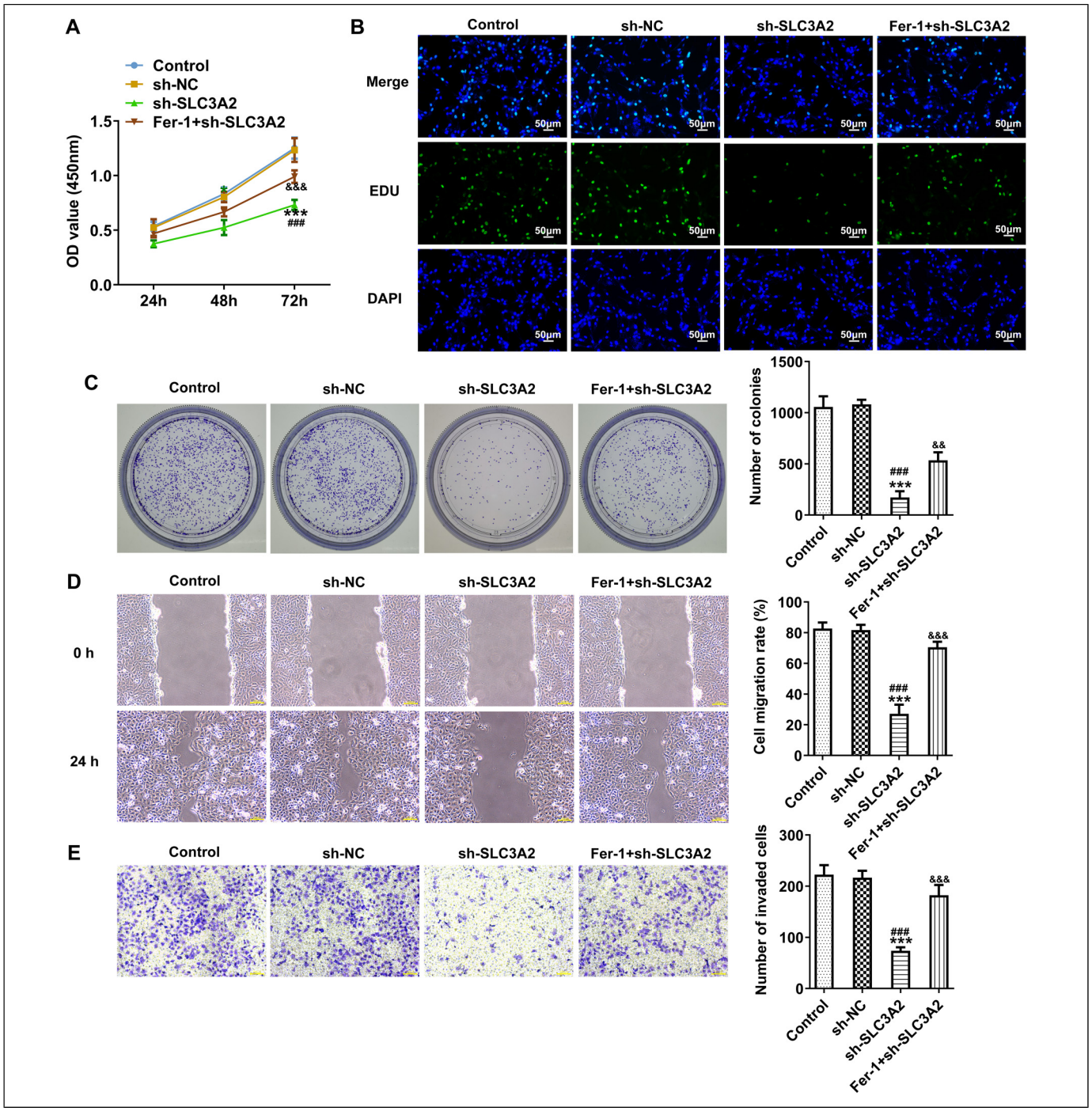

Figure 5. Interference with SLC3A2 inhibits BLCA cell proliferation, invasive, and migration by promoting ferroptosis. Cell proliferation detection by CCK8 assay (A, n = 5). Cell proliferation detection by EDU staining (B, n = 3). Cell proliferation detection by Colony formation assay (C, n = 3). Cell migration detection by wound healing assay (D, n = 5). Cell invasion detection by Transwell assay (E, n = 5). $^{***}P < .001$ versus control; $^{\#\#\#}P < .001$ versus sh-NC; $^{\&\&\&}P < .001$ versus Fer-1 + sh-SLC3A2. Abbreviations: BLCA, bladder cancer; EDU, 5-ethynyl-2-deoxyuridine.

SLC3A2 regulates the proliferation, invasion, and migration of T24 BLCA cells.

Macrophages constitute a crucial component of the TME. M1-type macrophages predominantly inhabit chronic inflammatory sites where tumors initiate and develop, exerting an inhibitory role tumor growth.[23] In contrast, M2-type macrophages promote malignant tumor progression by inducing immunosuppression and microenvironmental remodeling.[24] The correlation and role of SLC3A2 in various tumors have been extensively researched, including its reported influence

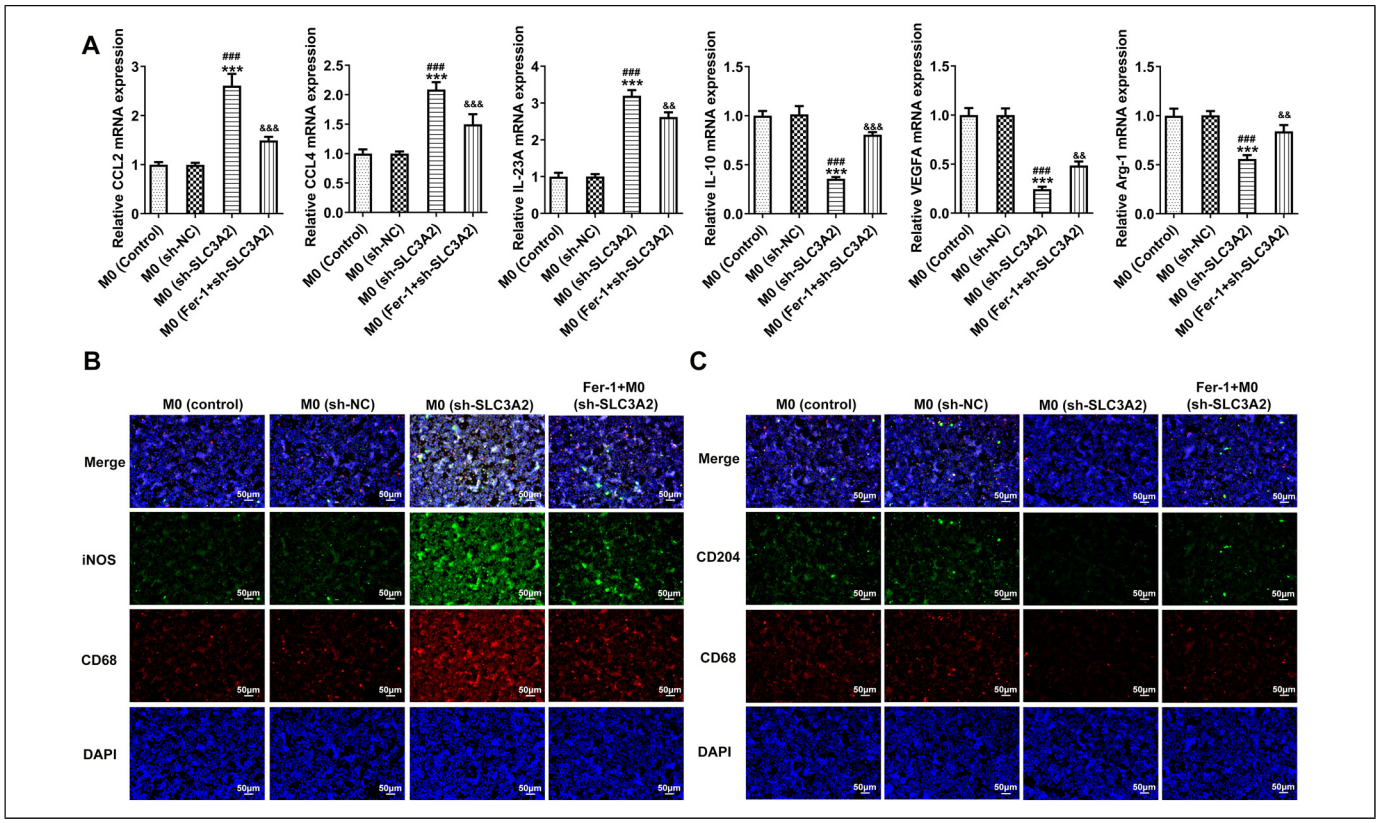

Figure 6. Interference with SLC3A2 inhibits M2-type polarization of tumor-associated macrophages by promoting ferroptosis. M1 and M2 type markers expression in macrophages after CM stimulation (A, n = 3). Double immunofluorescence staining of M1 macrophage markers after CM stimulation (B, n = 3). Double immunofluorescence staining of M2 macrophage markers after CM stimulation (C, n = 3). $^{***}P < .001$ versus control; $^{\#\#\#}P < .001$ versus sh-NC; $^{\&\&}P < .01$; $^{\&\&\&}P < .001$ versus Fer-1 + sh-SLC3A2. Abbreviation: CM, conditioned medium.

on cancer cell proliferation by regulating macrophage polarization. Li et al[16] reported that SLC3A2 promotes the polarization of tumor-associated macrophages in lung adenocarcinoma, and its mechanism is related to regulating metabolic reprogramming in lung cancer. Our study revealed a notable reduction in the expression of M2-like differentiation markers in M0 macrophages following stimulation with CM from sh-SLC3A2 group T24 cells. This suggests that SLC3A2 plays a role in regulating the polarization of tumor-associated macrophages in primary BLCA cells. In contrast to the findings of Li et al, SLC3A2 regulates macrophage polarization through ferroptosis mediation in T24 BLCA cells. This offers a new perspective for fully understanding the mechanism of SLC3A2 in tumor-associated macrophage polarization.

Currently, numerous studies have confirmed the relationship between ferroptosis, tumor, and the TME.[25,26] Ferroptosis, identified as a form of regulated cell death, depends on iron and ROS.[27] SLC7A11 and FTH1 are common inhibitors of ferroptosis, while ACSL4 and TFR1 act as positive regulators of ferroptosis and promote ferroptosis.[28,29] Interfering with SLC3A2 expression in BLCA cells significantly increased lipid ROS, lipid peroxidation, and Fe^{2+} levels, upregulating the expression of pro-ferroptosis factor proteins and downregulating the expression of antiferroptosis proteins in BLCA cells. These results suggest that interfering with SLC3A2 promotes ferroptosis in BLCA cells, suggesting the involvement of ferroptosis in BLCA progression. Additionally, the inhibitory effects of SLC3A2 interference on BLCA cell growth and M2-type macrophage polarization were significantly attenuated by the addition of ferroptosis inhibitors. These effects of SLC3A2 inhibition were mediated by ferroptosis.

However, there are still some limitations in the current research. Firstly, this study only focused on the T24 BLCA cells. However, in preliminary experiments, it was found that SLC3A2 was highly expressed in various BLCA cells. This suggests that SLC3A2 may play a role in other BLCA cell lines, indicating the need for a broader study involving different types of cells. Secondly, the findings of this study are restricted to the cellular level. It is important to note that cells may lose some of their original biological characteristics during passage culture, and the in vitro culture environment may not fully represent the in vivo environment. Therefore, it is necessary to further confirm the role of interfering with SLC3A2 in BLCA growth in vivo by constructing a tumor-bearing mouse model. Additionally, in the experiment on macrophage differentiation, it was found that interfering with SLC3A2 promotes ferroptosis and inhibits M2 polarization. However, the specific

mechanism by which interfering with SLC3A2 affects macrophage polarization in BLCA is complex. It is still unclear which substance in the CM causes the change in macrophage polarization, and further in-depth research is needed to explore both the substance and the underlying mechanism. For instance, Li et al[16] discovered that SLC3A2 facilitates the polarization of macrophages in lung adenocarcinoma by regulating arachidonic acid. This finding may offer valuable insights for future research. Lastly, ferroptosis involves complex molecular mechanisms. For instance, SLC3A2 regulates ferroptosis in laryngeal cancer through the mammalian target of rapamycin (mTOR) pathway.[30] Therefore, further exploration is needed to understand the mechanisms by which interfering with SLC3A2 promotes ferroptosis and exerts its effects.

In conclusion, this investigation revealed the role of SLC3A2 in the T24 cells of primary BLCA. SLC3A2 functions as an oncogene in BLCA. Interference with SLC3A2 impedes the growth of T24 BLCA cells and the M2-type polarization of tumor-associated macrophages by promoting ferroptosis. This study offers a theoretical reference for comprehending the role of SLC3A2 in BLCA and the mechanism for regulating macrophage differentiation.

Availability of Data and Materials

The datasets generated for this study are available on request to the corresponding author.

Authors' Contributions

All authors contributed to the study conception and design. Material preparation, data collection and analysis were performed by PW, LZ, and GK. The first draft of the manuscript was written by PW and SB. All authors commented on previous versions of the manuscript. All authors read and approved the final manuscript.

Declaration of Conflicting Interests

The authors declared no potential conflicts of interest with respect to the research, authorship, and/or publication of this article.

Funding

The authors received no financial support for the research, authorship, and/or publication of this article.

ORCID iD

Bo Song https://orcid.org/0009-0007-9510-2681

References

1. Lenis AT, Lec PM, Chamie K, Mshs MD. Bladder cancer: a review. *JAMA*. 2020;324(19):1980-1991.
2. Tan S, Kang Y, Li H, et al. circST6GALNAC6 suppresses bladder cancer metastasis by sponging miR-200a-3p to modulate the STMN1/EMT axis. *Cell Death Dis*. 2021;12(2):168.
3. Compérat E, Amin MB, Cathomas R, et al. Current best practice for bladder cancer: a narrative review of diagnostics and treatments. *Lancet*. 2022;400(10364):1712-1721.
4. Wang S, Zhang G, Zheng W, et al. MiR-454-3p and miR-374b-5p suppress migration and invasion of bladder cancer cells through targetting ZEB2. *Biosci Rep*. 2018;38(6):BSR20181436.
5. Griffiths TR. Current perspectives in bladder cancer management. *Int J Clin Pract*. 2013;67(5):435-448.
6. Wang JJ, Lei KF, Han F. Tumor microenvironment: recent advances in various cancer treatments. *Eur Rev Med Pharmacol Sci*. 2018;22(12):3855-3864.
7. Xiao Y, Yu D. Tumor microenvironment as a therapeutic target in cancer. *Pharmacol Ther*. 2021;221:107753.
8. Ricketts TD, Prieto-Dominguez N, Gowda PS, Ubil E. Mechanisms of macrophage plasticity in the tumor environment: manipulating activation state to improve outcomes. *Front Immunol*. 2021;12:642285.
9. Pan Y, Yu Y, Wang X, Zhang T. Tumor-associated macrophages in tumor immunity. *Front Immunol*. 2020;11:583084.
10. Bano I, Horky P, Abbas SQ, et al. Ferroptosis: a new road towards cancer management. *Molecules*. 2022;27(7):2129.
11. Zeng F, Lan Y, Wang N, Huang X, Zhou Q, Wang Y. Ferroptosis: a new therapeutic target for bladder cancer. *Front Pharmacol*. 2022;13:1043283.
12. Hao X, Zheng Z, Liu H, et al. Inhibition of APOC1 promotes the transformation of M2 into M1 macrophages via the ferroptosis pathway and enhances anti-PD1 immunotherapy in hepatocellular carcinoma based on single-cell RNA sequencing. *Redox Biol*. 2022;56:102463.
13. Chen P, Wang D, Xiao T, et al. ACSL4 promotes ferroptosis and M1 macrophage polarization to regulate the tumorigenesis of nasopharyngeal carcinoma. *Int Immunopharmacol*. 2023;122:110629.
14. Yang Y, Wang Y, Guo L, Gao W, Tang TL, Yan M. Interaction between macrophages and ferroptosis. *Cell Death Dis*. 2022;13(4):355.
15. He J, Liu D, Liu M, Tang R, Zhang D. Characterizing the role of SLC3A2 in the molecular landscape and immune microenvironment across human tumors. *Front Mol Biosci*. 2022;9:961410.
16. Li Z, Chen S, He X, Gong S, Sun L, Weng L. SLC3A2 Promotes tumor-associated macrophage polarization through metabolic reprogramming in lung cancer. *Cancer Sci*. 2023;114(6):2306-2317.
17. Huang G, Ma L, Shen L, et al. MIF/SCL3A2 depletion inhibits the proliferation and metastasis of colorectal cancer cells via the AKT/GSK-3β pathway and cell iron death. *J Cell Mol Med*. 2022;26(12):3410-3422.
18. Xiao Y, Xu D, Jiang C, et al. Telomere maintenance-related genes are important for survival prediction and subtype identification in bladder cancer. *Front Genet*. 2022;13:1087246.
19. Liu R, Sun X, Hu Z, Peng C, Wu T. Knockdown of long non-coding RNA MIR155HG suppresses melanoma cell proliferation, and deregulated MIR155HG in melanoma is associated with M1/M2 balance and macrophage infiltration. *Cells Dev*. 2022;170:203768.
20. Liu B, Lv Y, Hu W, et al. M(6)A modification mediates SLC3A2/SLC7A5 translation in 3-methylcholanthrene-induced uroepithelial transformation. *Cell Biol Toxicol*. 2024;40(1):5.
21. Hirotsu Y, Yokoyama H, Amemiya K, et al. Genomic profile of urine has high diagnostic sensitivity compared to cytology in non-invasive urothelial bladder cancer. *Cancer Sci*. 2019;110(10):3235-3243.

22. Liang Y, Zhu J, Huang H, et al. SESN2/sestrin 2 induction-mediated autophagy and inhibitory effect of isorhapontigenin (ISO) on human bladder cancers. *Autophagy*. 2016;12(8): 1229-1239.
23. Moyano A, Ferressini Gerpe NM, De Matteo E, Preciado MV, Chabay P. M1 macrophage polarization prevails in Epstein-Barr virus-infected children in an immunoregulatory environment. *J Virol*. 2022;96(1):e0143421.
24. Liu L, Zhou X, Cheng S, et al. RNA-binding protein DHX9 promotes glioma growth and tumor-associated macrophages infiltration via TCF12. *CNS Neurosci Ther*. 2023;29(4): 988-999.
25. Zhao L, Zhou X, Xie F, et al. Ferroptosis in cancer and cancer immunotherapy. *Cancer Commun (Lond)*. 2022;42(2): 88-116.
26. Mou Y, Wang J, Wu J, et al. Ferroptosis, a new form of cell death: opportunities and challenges in cancer. *J Hematol Oncol*. 2019;12(1):34.
27. Tang D, Chen X, Kang R, Kroemer G. Ferroptosis: molecular mechanisms and health implications. *Cell Res*. 2021;31(2):107-125.
28. Xu J, Wang XL, Zeng HF, Han ZY. Methionine alleviates heat stress-induced ferroptosis in bovine mammary epithelial cells through the Nrf2 pathway. *Ecotoxicol Environ Saf*. 2023; 256:114889.
29. Liu H, Zhao Z, Yan M, Zhang Q, Jiang T, Xue J. Calycosin decreases cerebral ischemia/reperfusion injury by suppressing ACSL4-dependent ferroptosis. *Arch Biochem Biophys*. 2023;734:109488.
30. Wu F, Xiong G, Chen Z, Lei C, Liu Q, Bai Y. SLC3A2 Inhibits ferroptosis in laryngeal carcinoma via mTOR pathway. *Hereditas*. 2022;159(1):6.